Supporting Information

PEGylation Improved Electrochemiluminescence Supramolecular Assembly of Iridium (III) Complexes in Apoferritin for Immunoassay Using 2D/2D MXene/TiO_2 Hybrids as Signal Amplifiers

Lei Yang,[†, §] Tingting Wu,[†, §] Yu Du,*[,‡] Nuo Zhang,[†] Ruiqing Feng,*[,†] Hongmin Ma,[†, ‡] and Qin Wei [†,‡]

[†] Key Laboratory of Interfacial Reaction & Sensing Analysis in Universities of Shandong, School of Chemistry and Chemical Engineering, University of Jinan, Jinan 250022, PR China.

[‡]Collaborative Innovation Center for Green Chemical Manufacturing and Accurate Detection of Shandong Province, University of Jinan, Jinan 250022, PR China.

*** Corresponding author**

Tel.: +86 531 82765730;

Fax: +86 531 82765969;

E-mail: duyu_ujn@163.com (Y. Du), fengruiqingsx@163.com (R. Feng).

Contents:

S1. Materials, reagents, and apparatus.

$Ti_3C_2T_x$ MXenes product was purchased from XFNano Materials Tech Co., Ltd (Nanjing, China). Gold chloride tetrahydrate ($HAuCl_4 \cdot 4H_2O$), horse spleen apoferritin (100 mg/mL), bovine serum albumin (BSA) (96–99%), and $Ir(ppy)_2(acac)$ (ppy = 2-phenylpyridine, acac= acetylacetonate) were purchased from Sigma-Aldrich Co. (St. Louis, MO, USA). NHS-PEG-NHS (2000) was purchased from Ponsure Biological Company (Shanghai, China). The sodium borohydride ($NaBH_4$), tetra-n-butylammonium hexafluorophosphate ($TBAPF_6$) and tetrahydrofuran (THF) were obtained from Shanghai Reagent Company (Shanghai, China). The capture-antibody (Ab_1), detection antibody (Ab_2) and antigen of Neuron Specific Enolase (NSE), antigens of CYFRA 21-1, CEA, and CA125 were all purchased from Shanghai Linc-Bio Science Co. LTD (Shanghai, China). All the other chemicals were of analytical reagent grade and were used without further purification. Phosphate buffered saline (PBS) was prepared by using 0.1 M Na_2HPO_4 and 0.1 M KH_2PO_4 solution and nitrogen bubbled for 30 min to eliminate the dissolved O_2. 5 mmol/L of $K_3Fe(CN)_6/K_4Fe(CN)_6$ and 0.1 mol/L of KCl solution were used as electrolyte for electrochemical impedance spectroscopy (EIS). Deionized water (18.25 MΩ/cm, 20 °C) was used for all the experiments.

Transmission electron microscope (TEM) and high resolution TEM (HRTEM) images were obtained by JEOL JEM-2100F (Japan). Dynamic Light Scattering (DLS) and zeta-potential was obtained from the Zetasizer Nano ZS 90 (Malvern, U.K.). The UV-vis absorption result was acquired by TU-1909 spectrophotometer (Beijing Puxi Instrument

Co. Ltd, China). ICP-OES tests were conducted by Agilent 720ES. Circular dichroism (CD) spectrum was obtained by Applied Photophysics. Ltd (Britain). Electron spin resonance (ESR) spectra was obtained by Bruker EMX Plus (Germany).

The ECL spectrum analyzer consisting of an Acton SP2300i mono-chromator equipped with a liquid N_2-cooled PyLoN 400BReXcelon digital charge-coupled device (CCD) detector (Princeton Instruments) and a VersaSTAT 3 electrochemical analyzer (Princeton Applied Research). For spectra comparison, the ECL and FL spectra were obtained on CHI 660D electrochemical workstation with a F-7000 fluorescence spectrometer.

S2. DLS, CD, TEM, UV-vis, and ECL measurements.

Dynamic Light Scattering Analysis. Dynamic light scattering (DLS) analysis was measured using a Zetasizer Nano ZS90 instrument (Malvern, U.K.). Before measurement, the samples were diluted to ~0.5 mg/mL and further centrifuged at 10 000 for 10 min and equilibrated to 25 °C.

Circular Dichroism Spectroscopy. Circular dichroism (CD) spectrum was conducted on a J-1500 spectrometer (Jasco, Tokyo, Japan) to monitor the conformational changes of apoHSF during the preparation of Ir@PEG-apoHSF. All the CD spectra were recorded in a quartz cuvettes of 1 mm optical path length, which were taken as the average of three accumulations from 190 and 300 nm at a speed of 200 nm/min and a bandwidth of 5.0 nm.

Transmission Electron Microscope. Transmission electron microscope (TEM) was performed by JEOL JEM-2100F (Japan). 10 μL pure PEG-apoHSF and Ir@PEG-apoHSF were dropped onto three carbon-coated copper microgrids for 5 min at room temperature and the excess solution was removed by using filter paper. For negative staining TEM, additional 5 μL of 2% uranyl acetate was dropped onto the moist grids for negative staining and dried in vacuum.

UV−vis absorption spectroscopy. For UV–vis absorption study, the PEG-apoHSF and Ir@PEG-apoHSF samples with same apoHSF concentration of 0.5 mg/mL, and $Ir(ppy)_2(acac)$ suspension with a concentration of 3 mg/mL were dispersed in PBS (0.1

mol/L, pH 7.4). All the spectra were recorded by a TU-1909 spectrophotometer (Beijing Puxi Instrument Co. Ltd, China). The scan was set in the range from 200 to 500 nm with a speed of 300 nm/min at at room temperature. All data were collected in triplicate.

ECL Measurements. The ECL measurements were performed with an MPI-E ECL Analyzer (Xi'an remax Electronic Science Tech. Co. Ltd., China), electrochemical measurements were carried out on electrochemical workstation (Zahner Zennium PP211, Germany) using a three-electrode system which includes a platinum wire as an auxiliary electrode, an Ag/AgCl electrode as reference electrode, and GCE (4 mm in diameter) as working electrode.

S3. Elemental mapping of $Ti_3C_2T_x/TiO_2$ hybrids

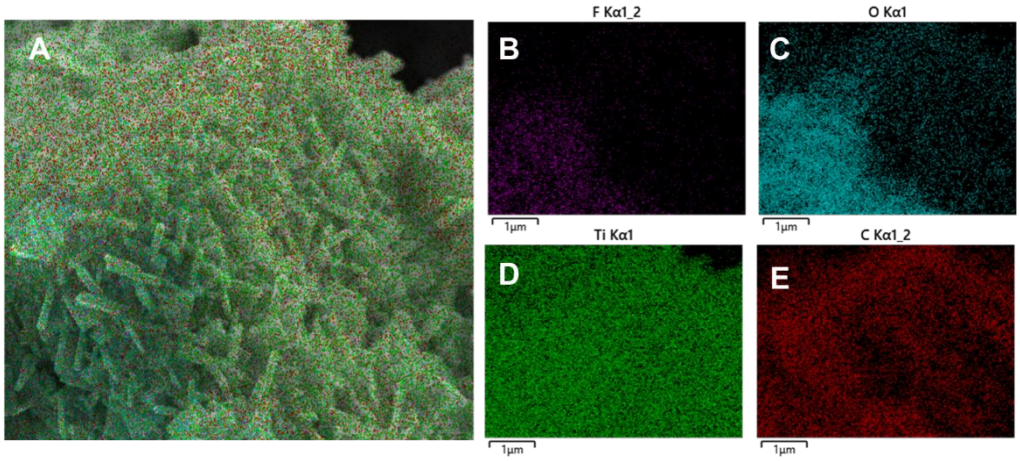

Figure S1. Elemental mapping spectra (A-E) of F, O, Ti, and C elements of $Ti_3C_2T_x/TiO_2$ hybrids.

S4. Negative stained TEM image of PEG-apoHSF

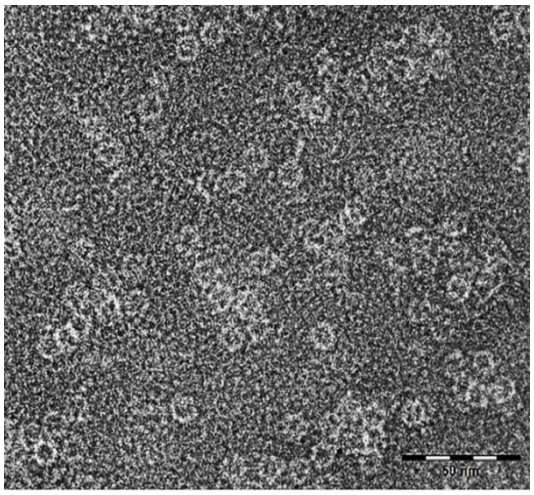

Figure S2. Negative stained TEM image of PEG-apoHSF.

S5. ICP-OES analyses.

As comparison, apoHSF without PEGylation was also used to prepare the Ir@apoHSF nanodots. The total Ir contents of 1 mL of prepared Ir@PEG-apoHSF and Ir@apoHSF were quantified by using ICP-OES. All the samples were 10 times diluted before ICP-OES analysis. The linear equation was determined as y= 1744 $\times c$ + 8.7, R^2 = 0.992. The results were listed in **Table S1** and **S2**.

Table S1. The Ir contents of Ir@PEG-apoHSF samples of different batches, n = 5

Batch number	ICP-OES intensity	Instrument reading C (μg /mL)	Volume (mL)	Ir contents (μg)	Average contents (μg)	Total contents (mg)
1	7734.62	4.43		44.3		
2	8065.98	4.62		46.2		
3	7385.82	4.23	10	42.3	43.5	0.218
4	7298.62	4.18		41.8		
5	7525.34	4.31		43.1		

Table S2. The Ir contents of Ir@apoHSF samples of different batches, n = 5

Batch number	ICP-OES intensity	Instrument reading C (μg /mL)	Volume (mL)	Ir contents (μg)	Average contents (μg)	Total contents (mg)
1	5519.74	3.16		31.6		
2	5868.74	3.36		33.6		
3	5415.10	3.10	10	31.0	32.2	0.161
4	5729.02	3.28		32.8		
5	5606.94	3.21		32.1		

The encapsulation efficiency (%) of iridium complexes in apoHSF was calculated according to the equations as follow:

Encapsulation efficiency (%) = weight of encapsulated iridium complexes (mg) / weight of added iridium complexes (mg) ×100% (1)

S6. ESR measurements

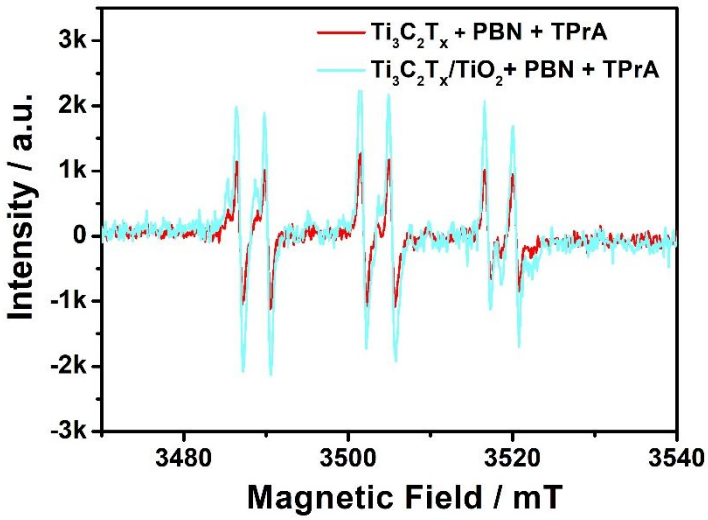

Figure S3. The ESR spectra of TPrA$^{\bullet}$ radicals captured by PBN in samples mixed with $Ti_3C_2T_x$ MXenes (red curve) and $Ti_3C_2T_x/TiO_2$ hybrids (cyan curve).

S7. ECL and FL spectra of $Ir(ppy)_2(acac)$

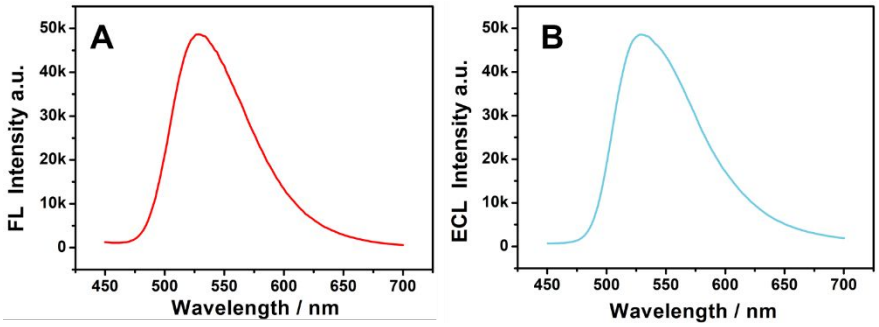

Figure S4. The FL (A) and ECL (B) spectra of $Ir(ppy)_2(acac)$ samples of same concentration (0.05 mmol/L). For FL spectra, the excitation wavelength was set as 320 nm, and the scanning range was 450 – 700 nm. For ECL spectra, the scanning potential was set as 0 –1.10 V with a scanning rate of 0.1 V/s in the range of 450 – 700 nm.

S8. CV measurements

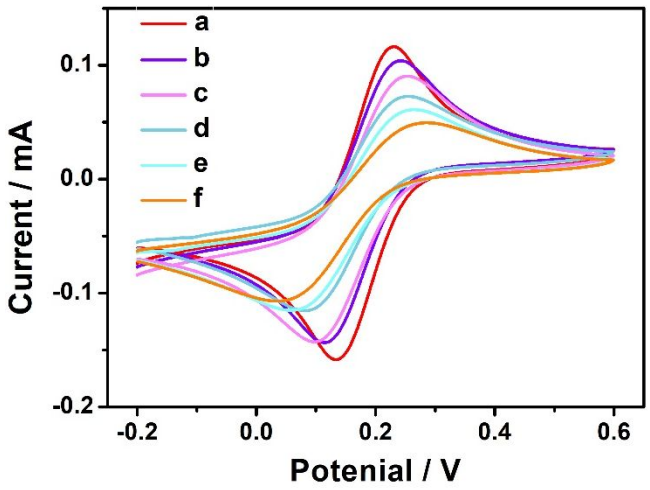

Figure S5. CV of (a) GCE/DpAu; (b) GCE/DpAu/$Ti_3C_2T_x$/TiO_2; (c) GCE/DpAu/$Ti_3C_2T_x$/TiO_2/Ab_1; (d) GCE/DpAu/$Ti_3C_2T_x$/TiO_2/Ab_1/BSA; (e) GCE/ DpAu/$Ti_3C_2T_x$/TiO_2/Ab_1/BSA/Ag; (f) GCE/DpAu/$Ti_3C_2T_x$/TiO_2/Ab_1/BSA/Ag/Ab_2-Ir@PEG-apoHSF modified electrodes in PBS containing 5.0 mmol/L $[Fe(CN)_6]^{-3/-4}$ solution and 0.1 mol/L KCL.

All the CV measurements were carried out on electrochemical workstation (Zahner Zennium PP211, Germany), which were in good agreements with EIS data. Therefore, it can be inferred that the layer-by-layer assembly process of the immunosensor was successful conducted.

S9. Optimization of experimental conditions

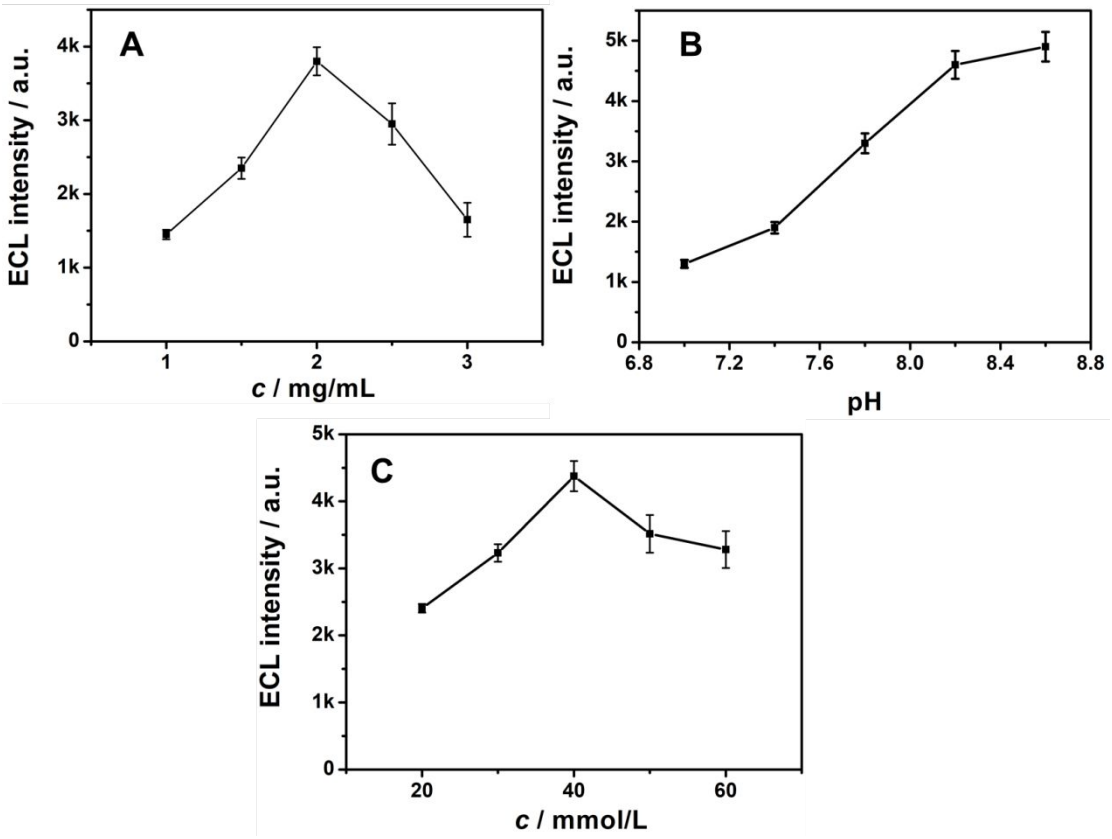

Figure S6. Optimization of $Ti_3C_2T_x/TiO_2$ concentration (A), pH value of PBS solution (B), and TPrA concentration (C).

To achieve better performance of the proposed ECL immunosensor, experimental conditions including $Ti_3C_2T_x/TiO_2$ concentration, pH value of PBS solution (B), and TPrA concentration were investigated orderly in this work. Because different concentrations of $Ti_3C_2T_x/TiO_2$ hybrids on the GCE surface will form different sensing substrates with various thickness, which might hinder the interfacial mass and electron transfer during the ECL process. Therefore, different concentrations of $Ti_3C_2T_x/TiO_2$

hybrids (1 mg/mL, 1.5 mg/mL, 2 mg/mL, 2.5 mg/mL, and 3 mg/mL) were separately modified onto bare GCE as the substrate to construct the sensor for detecting 1 ng/mL of antigen in PBS (0.1 mol/L, pH 7.4) containing 30 mmol/L TPrA. As shown in Figure S6A, it can included that the maximum ECL intensity of sensor was achieved at 2 mg/mL, indicting the formed sensing layer was most suitable for detecting antigen. On this basis, the ECL performance of constructed sensor for detecting 1 ng/mL of antigen was further optimized in PBS solution with different pH values (7.0, 7.4, 7.8, 8.2, and 8.6) in Figure S6B. Despite that alkaline environment was beneficial for the deprotonation of $TPrA^+$, the pH of the used electrolytes should be biocompatible for maintaining the bioactivity of the biomolecules on the sensing interface. After weighing and balancing the ECL signal out-put of the immunosensor and bioactivity maintenance for biomolecules, pH 7.8 was finally chosen as the optimal value for following study. Finally, the ECL performance of constructed sensor for detecting 1 ng/mL of antigen was optimized in PBS (0.1 mol/L, pH 7.8) containing different TPrA concentration (20, 30, 40, 50, and 60 mmol/L). As shown in Figure S6C, the ECL maximum intensity was obtained in 40 mmol/L of TPrA for the following study.

S10. Comparison of different methods for NSE detection

Table S3. Comparison of different methods for NSE detection

Methods	Linear range (ng/mL)	LOD (pg/mL)	Reference
Molecularly-imprinted electrochemical assay	0.01-1.0	2.6	1
Photoelectrochemical immunoassay	0.005 – 1.5	3.5	2
Surface-Enhanced Raman Scattering assay	1.0 - 75.0	860	3
Electrochemical assay	0.001 - 100	0.483	4
Electrochemiluminescence assay	0.0001 – 50	0.035	This work

Reference

(1) Wang, X.; Wang, Y.; Ye, X.; Wu, T.; Deng, H.; Wu, P.; Li, C., Sensing Platform for Neuron Specific Enolase based on Molecularly Imprinted Polymerized Ionic Liquids in between Gold Nanoarrays. *Biosens, Bioelectron.* 2018, *99*, 34-39.

(2) Liu, R.; Wang, Y.; Wong, W.; Li, H.; Li, C., Photoelectrochemical Immunoassay Platform based on MoS_2 Nanosheets Integrated with Gold Nanostars for Neuron-Specific Enolase Assay. *Microchim. Acta.* 2020, *187*, 480.

(3) Gao, X.; Zheng, P.; Kasani, S.; Wu, S.; Yang, F.; Lewis, S.; Nayeem, S.; Engler-Chiurazzi, E. B.; Wigginton, J. G.; Simpkins, J. W.; Wu, N., Paper-Based Surface-Enhanced Raman Scattering

Lateral Flow Strip for Detection of Neuron-Specific Enolase in Blood Plasma. *Anal. Chem.* **2017,** *89* (18), 10104-10110.

(4) Yin, S.; Zhao, L.; Ma, Z., Label-Free Electrochemical Immunosensor for Ultrasensitive Detection of Neuron-Specific Enolase based on Enzyme-Free Catalytic Amplification. *Anal. Bioanal. Chem.* **2018,** *410*, 1279-1286.

S11. *Inter*-assay precision of the immunosensor

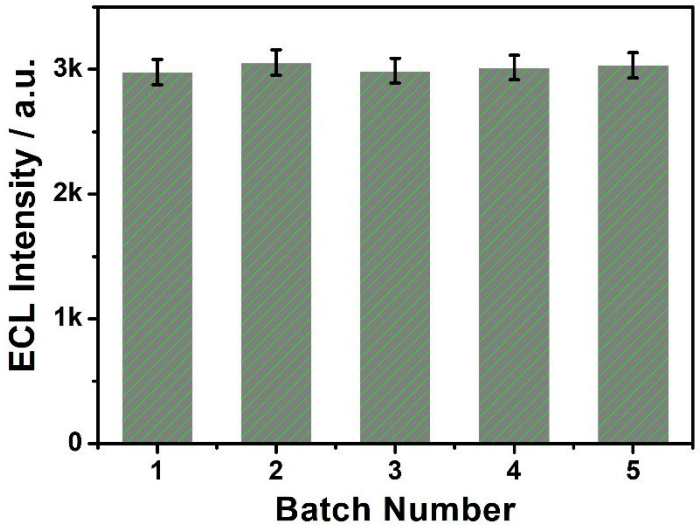

Figure S7. *Inter*-assay of same electrode in five different batches. Error bars = ± SD, *n* = 5.